



**POLITECNICO**  
**MILANO 1863**

# Project Report - Team 1

**ADDITIVE MANUFACTURING FOR SPACE APPLICATIONS**  
**MECHANICAL ENGINEERING**

Authors:

**11101078 Michal Zawadzki**  
**10770254 Michele di Nunzio**  
**11076681 Mantas Kazenas**  
**10956103 Martín Villacreses**

Lecturer: Prof. Tommaso Ghidini

Assistants: Yassir Ben Dahou, Giulio Valenti

Academic Year: 2024-25

# Contents

<b>Contents</b>	<b>i</b>
<b>1 Introduction</b>	<b>1</b>
<b>2 Topology Optimization</b>	<b>2</b>
2.1 Design space and preserved regions . . . . .	2
2.2 Load cases and boundary conditions . . . . .	3
2.3 Optimization objective and constraints . . . . .	5
2.4 Final optimized geometry . . . . .	6
2.5 Performance Summary after Optimization . . . . .	6
<b>3 Design for Additive Manufacturing</b>	<b>9</b>
3.1 Build orientation Selection . . . . .	9
3.2 Custom Support Structure Strategy . . . . .	10
3.3 Manual Geometry Refinement . . . . .	14
3.4 Post-DfAM Performance Validation . . . . .	15
<b>4 Process Simulation</b>	<b>17</b>
4.1 Simulation Objectives . . . . .	17
4.2 Simulation Setup . . . . .	17
4.3 Deformation Results . . . . .	18
<b>5 Results Discussion and Conclusions</b>	<b>20</b>

# 1 | Introduction

Additive Manufacturing (AM) is rapidly transforming the design and production of components for aerospace and space applications. Its ability to enable lightweight, highly optimized geometries makes it particularly valuable in satellite systems, where every gram saved can improve efficiency, reduce launch costs, or enable additional payload. This project, conducted as part of the Additive Manufacturing for Space Applications course, focused on the redesign of a structural bracket for AM, with the aim of demonstrating an integrated workflow combining topology optimization, design for AM, and process simulation.

**The component under study is a support bracket for a mirror used in the high-resolution spectrometer aboard the FLEX satellite — ESA's Fluorescence Explorer mission.** FLEX is dedicated to monitoring vegetation health globally by measuring solar-induced chlorophyll fluorescence. The bracket supports a precision optical mirror and must ensure minimal deflection and high dynamic stability under stringent performance requirements.

Originally manufactured using CNC machining from an aluminium alloy, the bracket weighed 3.7 kg. **The goal of this redesign was to reduce its mass while meeting all structural requirements, and to optimize the geometry for laser beam powder bed fusion (LB-PBF) additive manufacturing.**

This report documents the full redesign process and highlights the methods, tools, and engineering decisions used to transform a conventionally machined part into an AM-optimized component suitable for a real-world space mission.

# 2 | Topology Optimization

The topology optimization phase was central to the redesign process, aiming to reduce the mass of the optical mirror bracket while satisfying the strict mechanical requirements of a spaceborne optical system. This was done in nTop, using static and dynamic performance criteria derived from mission constraints.

## 2.1. Design space and preserved regions

The topology optimization began with the definition of a suitable design space, constructed from the simplified “bulk” geometry provided in place of the original CAD model. Since the bracket interfaces with both the mirror and the satellite structure, it was critical to preserve key functional features to ensure mechanical compatibility and accurate load transmission. The design space was defined in nTop and split into design and non-design (frozen) regions.

The preserved (non-design) regions included:

- **Eight mirror mounting holes** located at the front face of the bracket, representing the connection points to the optical assembly. These holes were retained to apply loads and simulate the effect of the mirror mass.
- **Four satellite interface holes** at the rear face, corresponding to the attachment points between the bracket and the spacecraft structure.
- **A cable guide channel** located at the bottom center of the bracket, which had to remain unobstructed for routing electrical connections.

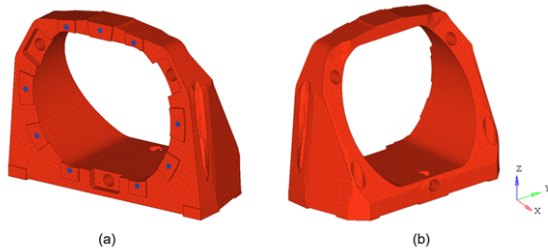
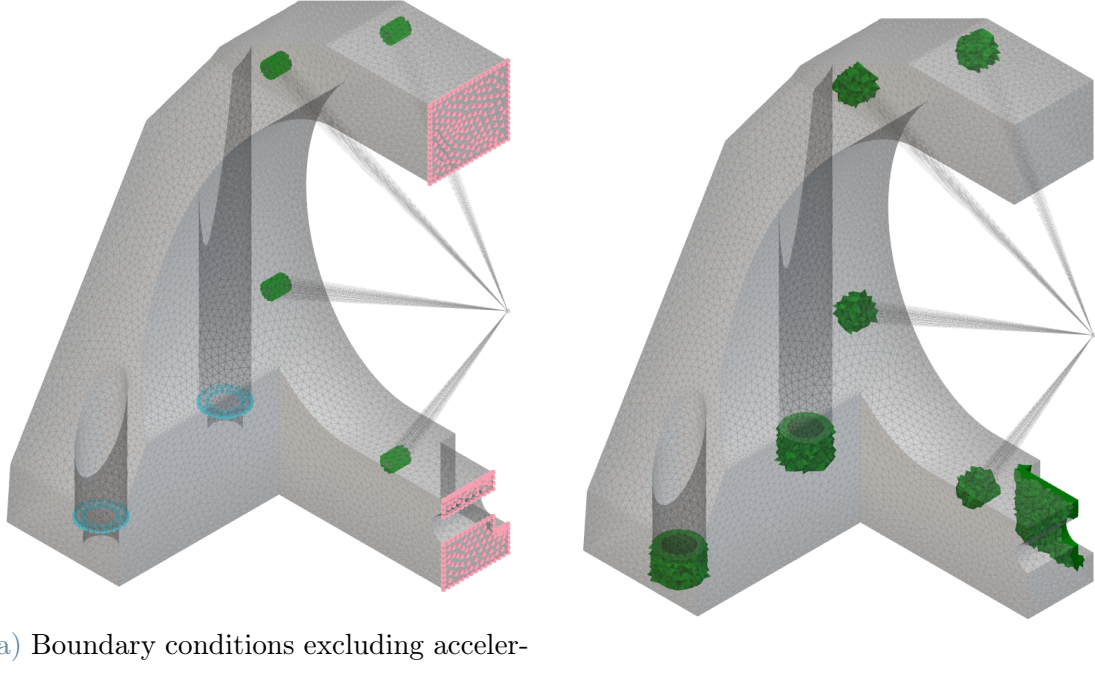


Figure 2.1: Design Space



(a) Boundary conditions excluding accelerations

(b) Preserved regions

Figure 2.2: Topology Optimization Setup; On the left: mirror inertial load (green), encastrate(blue), symmetry(red), and point mass (gray dot)

The rest of the volume surrounding these features was designated as the design region, where material could be added or removed freely by the optimization algorithm. Design freedom was maximized in this region to allow the solver to find structurally efficient geometries.

To enhance printability and simplify later post-processing, the model was also symmetrized along its central vertical plane in later iterations. This allowed for a higher-resolution mesh and a more stable optimization process without compromising design performance.

## 2.2. Load cases and boundary conditions

To ensure the redesigned bracket could meet its structural and dynamic requirements, multiple loading scenarios and appropriate boundary conditions were defined in nTop. These reflected both launch conditions and in-orbit performance needs, though only selected cases were included directly in the topology optimization phase.

### Quasi-Static Launch Load Cases

The primary structural loads were based on quasi-static accelerations expected during launch aboard the Vega-C vehicle. Four load cases were defined, corresponding to accelerations along different global directions:

Load case	X(g)	Y(g)	Z(g)
Acceleration 1	15	15	25
Acceleration 2	-15	15	25
Acceleration 3	15	-15	25
Acceleration 4	15	15	-25

Table 2.1: Load cases

Rather than modeling the mirror as a point mass in these cases, the team found that representing its inertial effects as equivalent force vectors applied directly to the eight front mounting holes led to faster and more stable optimization. These forces were scaled according to the mirror mass and the magnitude of each directional acceleration.

This simplification improved optimization speed and convergence, as it avoided the numerical complexity of mass-element coupling within the optimization solver, while still accurately distributing the launch loads.

### Gravity Load Case (Post-Check Only)

A separate load case simulating gravitational loading (1g) in the operational orientation was not used in the optimization itself but was applied later as part of performance verification. The primary objective of this post-check was to ensure that the mirror interface displacement remained below 5 micrometers, as required for preserving optical alignment in orbit.

### Dynamic Behavior – Natural Frequency Modeling

To evaluate and constrain the bracket dynamic response, the mirror was represented as a point mass (3.3 kg) located at the center of the mirror mounting interface. However, instead of using a rigid coupling, which artificially imposed infinite stiffness and led to nonphysical results, the connection was modeled with finite stiffness to reflect the real mechanical interface more accurately.

This flexible coupling allowed the optimization to account for the compliance of the bracket-mirror interface, ensuring that modal behavior was realistically captured. The resulting frequency estimates were therefore more representative of the true structural response, helping to enforce the requirement that the first eigenfrequency remain above 380 Hz.

### Boundary Conditions

The bracket was assumed to be fixed at its four bottom mounting holes, simulating a rigid attachment to the satellite structure. These constraints remained consistent across all load cases and were critical in shaping both the static response and dynamic behavior.

To further improve computational efficiency and allow for higher-resolution meshing, the design was assumed to be symmetric across a central vertical plane. As a result, only half of the bracket was included in the optimization domain. To enforce physical realism at the symmetry interface, the following symmetry boundary conditions were applied:

- Translation was restricted in the direction normal to the symmetry plane;

- **Rotations out of the plane** were also constrained;
- All other degrees of freedom remained free, allowing natural deformation and load flow in the design space.

This symmetry setup preserved design freedom while significantly reducing computational effort and aiding post-processing.

## 2.3. Optimization objective and constraints

The topology optimization process was formulated with the dual aim of minimizing the mass of the bracket while satisfying strict structural, dynamic, and manufacturability constraints. These were configured within nTop to guide the solver toward a geometry that could realistically be refined, fabricated, and flown.

**Objective Function** - The optimization objective was set to **minimize compliance** (i.e., maximize stiffness) under the four defined quasi-static load cases, corresponding to expected launch accelerations. Compliance minimization naturally favors material placement along load paths, which supports high structural efficiency.

**Volume Fraction Constraint** - A **volume constraint of 15%** of the original design space was applied. This encouraged aggressive material reduction while leaving enough flexibility for structural integrity and post-processing.

**Preserved Regions Constraint** - Geometric regions corresponding to mounting holes for the mirror and the satellite structure, as well as the cable routing area, were excluded from the design domain. These preserved regions ensured proper mechanical integration of the final design.

**Natural Frequency Constraint** - A dynamic constraint was applied to maintain a minimum first natural frequency of 380 Hz. To stabilize the solution and avoid local numerical artifacts, **the constraint considered the first five eigenmodes during optimization**. The mirror was modeled as a point mass with flexible coupling at the interface, allowing accurate representation of the bracket's modal behavior.

## Manufacturing-Oriented Constraints: Iterative Exploration

While the initial optimization run focused purely on performance, the resulting geometry presented significant challenges:

- The structure contained **thin, membrane-like surfaces**, which were difficult to post-process, especially when **voids or closed cavities** were present.
- Several features required **extensive support structures**, or trapped unmelted powder - both problematic for LB-PBF fabrication.

To address these issues, two different manufacturability constraints were tested:

**Overhang Constraint (45°)** - An overhang angle limit was introduced to promote **self-supporting geometry**. However, this constraint led to **significant degradation in**

**mechanical performance**, and the resulting geometry was visibly less efficient.

**Minimum Feature Size Constraint** - A minimum feature size of 10mm was then applied to penalize the formation of excessively thin surfaces. This approach proved much more effective:

- The resulting design transitioned to a **beam-like architecture**, inherently more suitable for AM.
- The geometry required **moderate post-processing** to reduce overhangs but was largely free of closed voids and unnecessary supports.
- Performance in both static and modal checks remained **comparable to the unconstrained solution**, validating the approach.

Ultimately, the **minimum feature size constraint** offered the best trade-off between structural efficiency and manufacturability, and was adopted for the final optimized design.

## 2.4. Final optimized geometry

The final bracket design was the outcome of an iterative optimization and validation process that carefully balanced structural performance, dynamic behavior, and additive manufacturability. The resulting geometry was both functionally efficient and almost AM-ready, shaped primarily by performance constraints and refined through post-processing.

### Geometry Overview

The final topology resembled a complex truss-based structure, with clearly defined load paths connecting the mirror interface to the satellite mounting holes. Material was **strategically concentrated near mounting interfaces**, where load transfer and stress concentrations are greatest, while the mid-span regions were minimized for weight savings. The design featured mostly beam-like elements, which avoided thin membranes and closed cavities and allowed for easier post-processing and powder removal.

Symmetry was preserved about the central plane, and the preserved regions for all functional interfaces — including the cable routing cutout — were fully retained throughout the optimization.

## 2.5. Performance Summary after Optimization

The optimized bracket underwent modal and static validation to confirm compliance with mission requirements:

**Final mass: 2.982 kg**, a -19.4% reduction from the original 3.7 kg CNC bracket.

**First natural frequency: 383 Hz**, the output cell density **threshold of at least 20%** was tuned to slightly exceed the minimum 380 Hz requirement, maximizing mass reduction without violating dynamic constraints.

**Static performance:**

Load Case	Peak Von Mises Stress [MPa]
1	6.14
2	5.84
3	6.57
4	6.16

Table 2.2: Results of quasi-static analysis

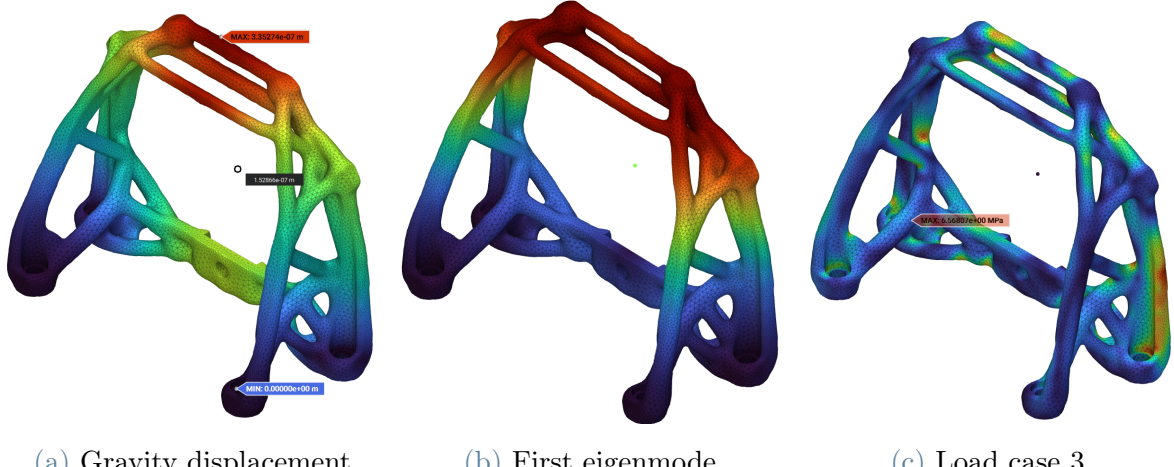


Figure 2.3: Results of quasi-static analysis

All values remained well below the yield strength of AlSi10Mg, confirming a robust design under launch accelerations.

**Gravity deflection check:** Under 1g loading in the operational orientation, **the maximum displacement of the whole mirror bracket was only 0.17  $\mu\text{m}$** , well below the 5  $\mu\text{m}$  limit for just mirror interface. This confirmed that the bracket provides excellent stiffness to maintain optical alignment, even under gravitational loads.

### Post-Processing

The raw output from topology optimization was smoothed using nTop's native tools. This removed surface noise and irregularities while preserving structural features. Boolean operations were then applied to cleanly merge the smoothed topology with preserved regions like bolt bosses and cable routing geometry. Further details on post-processing and manufacturability enhancements are covered in the next chapter.

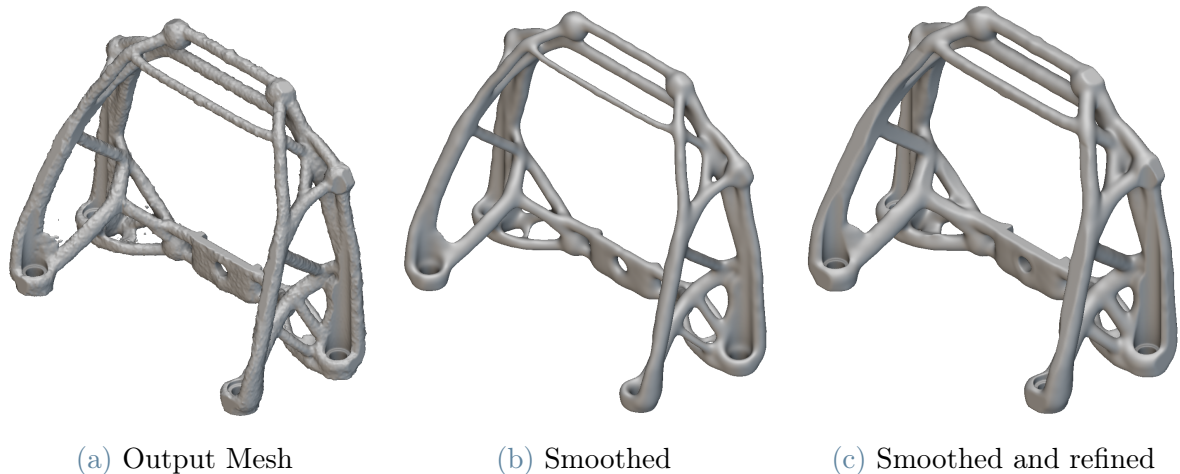


Figure 2.4: Topology Optimization results at various stages

# 3 | Design for Additive Manufacturing

## 3.1. Build orientation Selection

Choosing an appropriate build orientation was one of the most impactful decisions in preparing the bracket for additive manufacturing. The orientation influences support volume, thermal stress distribution, surface quality, and ultimately the mechanical integrity of the printed component.

### Final Orientation Strategy

After evaluating several options, the selected orientation placed the mirror interface directly on the build plate, positioning the part in a mostly horizontal configuration. This strategy was chosen primarily to:

- **Minimize support volume**, especially under the larger truss-like features and internal overhangs;
- **Reduce build height**, thus shortening print time and reducing thermal stress accumulation;
- **Preserve surface finish** at the satellite interface holes, which remained fully exposed and accessible;
- **Ensure easy support removal** from internal and recessed areas.

This approach positioned the **bulk of the bracket's mass close to the build plate**, improving heat dissipation and overall thermal stability during the build. However, the **two satellite mounting interfaces** located at the top of the part were expected to be **most prone to thermal distortion**, due to their height and isolation.

### Data-Driven Orientation Validation

To validate the choice of orientation, a **custom orientation evaluation workflow** was developed in nTop. The process involved:

- Randomly generating approximately 2000 unit vectors, each representing a different possible build direction;
- Rotating the part accordingly for each orientation;
- Automatically calculating the total support volume required for each case;

- Sorting the results to identify the orientation with the lowest support requirement.

The analysis confirmed that the horizontal orientation with the mirror interface facing down yielded the least support material, justifying its selection with quantitative evidence.

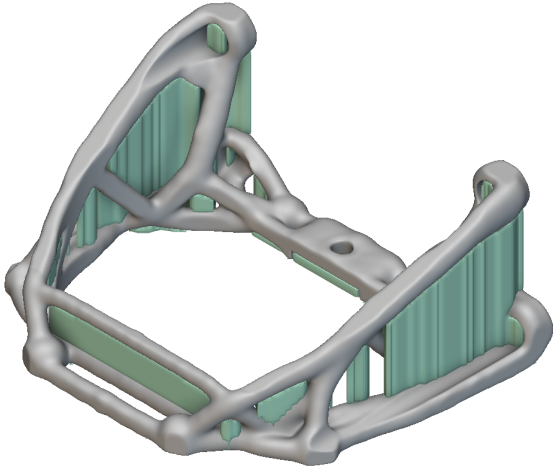


Figure 3.1: Minimum support orientation (Support volume in green)

### Alternative Orientations Considered

Two alternatives were explored:

1. **45° Tilt Orientation** - Provided a compromise between surface exposure and Z-height but introduced significant overhangs on the truss features, increasing support material requirements and surface roughness risk.
2. **Vertical Orientation (Satellite Interfaces Down)** - Resulted in the lowest distortion at the satellite interfaces but significantly increased the Z-height, leading to longer print times and higher internal thermal stresses.

These configurations were ultimately rejected in favor of the flatter orientation, which offered a better balance of manufacturability, thermal stability, and post-processing efficiency.

## 3.2. Custom Support Structure Strategy

The bracket's geometry, shaped by topology optimization, posed significant challenges for support generation. The organic truss-like structure included internal cavities, dense beams, and angled overhangs that conventional support algorithms struggled to handle effectively. To overcome this, we developed a custom support strategy in nTop that allowed full control over the support structure geometry, thermal anchoring behavior, and material efficiency.

## Initial Attempts and Limitations

We initially attempted to use Altair Inspire Print3D for automatic support generation. Our workflow involved:

- Using block supports for accessible surfaces;
- Applying tree supports where block supports would anchor to the top of the bracket instead of the build plate.

However, the tree support algorithm repeatedly positioned its roots on top of the part, even in areas where build plate anchoring was clearly feasible. With no access to modify the algorithm, we found these supports:

- Structurally suboptimal;
- Wasteful in material;
- Very difficult to remove without damaging the part.

This experience led us to abandon commercial auto-support features in favor of a custom, optimization-based support structure created in nTop.

## Support Design Space and Setup in nTop

The workflow involved the following steps:

1. **Identifying Overhang Regions** - We used nTop's Manufacturing Support Beams block to detect overhang surfaces exceeding a 45° threshold with respect to the build direction. Since the bracket is symmetric we only need to generate supports for one side and then mirror the results.
2. **Defining the Support Design Space** - From the detected overhang regions, we seeded a cloud of support anchor points, then:
  - Grew cones inclined at 45° from each point toward the build plate;
  - Boolean combined the cones into one solid volume;
  - Subtracted the bracket geometry, yielding a clean, custom support design space that reached from critical overhangs to the build plate.

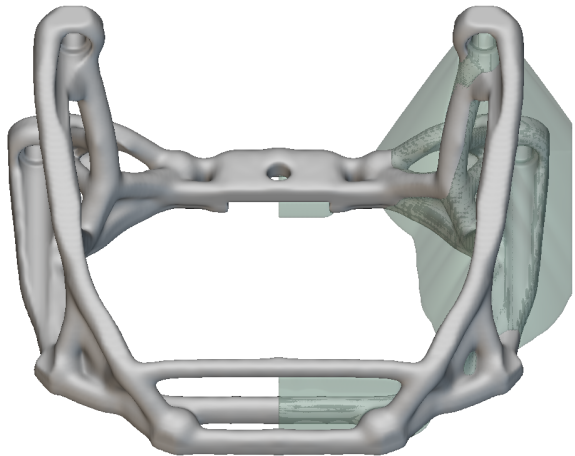


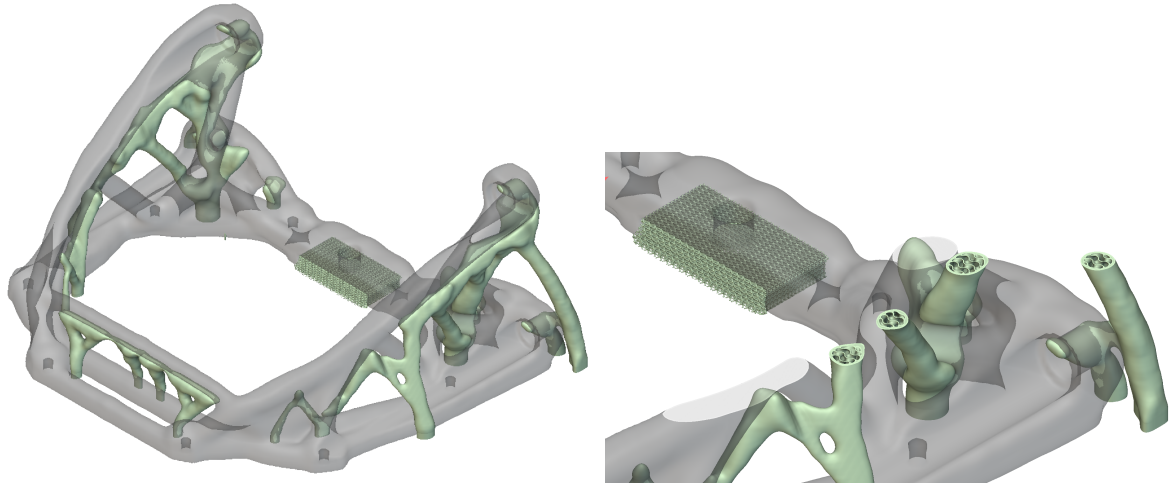
Figure 3.2: Support optimization design space

3. **Setting Up the Optimization Problem** - To generate the custom supports, we set up a topology optimization problem within the design space defined in the previous step. **The objective of the optimization was to minimize compliance of the support structure under gravity load** — in other words, to maximize its stiffness and resistance to sagging or thermal deformation during the build. All **faces in contact with the build plate were assigned fixed boundary conditions**, ensuring stable anchoring of the support structure. The **surfaces identified as requiring support were treated as preserved regions**, meaning they had to remain connected to the final support geometry and were not altered during optimization. A **gravitational acceleration field was applied across the entire design space** to simulate the effects of build-time self-weight, encouraging structurally efficient support paths.

To promote manufacturability and avoid overly bulky support forms, we included a **45° overhang constraint**, ensuring that the resulting geometry respected the minimum self-supporting angle of the process. This constraint also took into account the preserved overhang surfaces. In addition, we introduced a **maximum feature size constraint of 10 mm**, which penalized thick, monolithic volumes and encouraged branching, tree-like structures that are easier to post-process and require less material. This combination of objectives and constraints led to support geometries that were not only structurally effective but also well-suited for laser powder bed fusion processes.

4. **Post-processing** - To further improve material efficiency, the resulting solid support geometry was post-processed by applying a **shell operation** to create a hollow outer wall. The internal volume was then **filled with a gyroid lattice**, which maintained stiffness while significantly reducing material usage. This final support body was exported as a separate part and later combined with the bracket geometry for process simulation and build preparation.

The final supports were exported as a separate body and merged with the bracket model for process simulation and slicing.



(a) Supports overview

(b) Section cut of the supports

Figure 3.3: Supports made with topology optimization

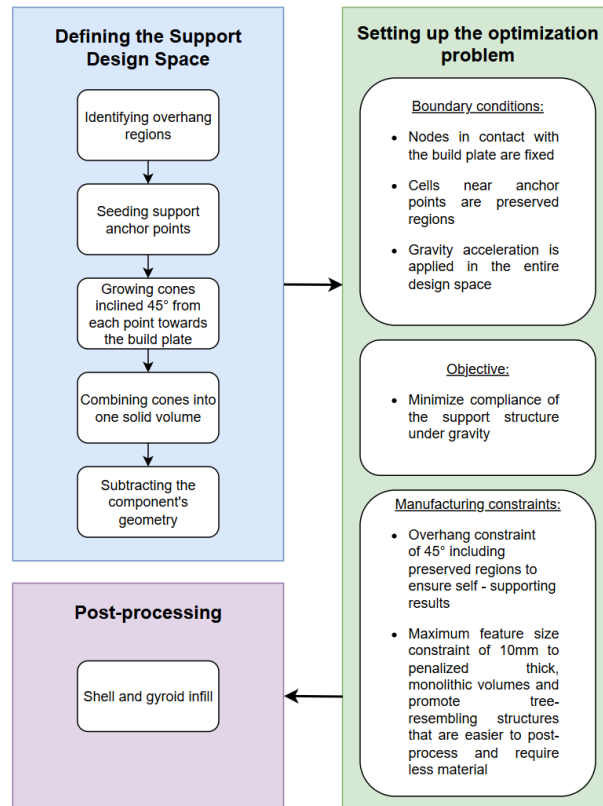


Figure 3.4: Block diagram of support generation workflow

## Advantages of the Custom Strategy

This approach offered several critical benefits over the default slicer supports:

- Precise placement of supports only where structurally needed;
- Anchoring always reached the build plate, never the component itself (although it could be altered if deemed beneficial);
- Gyroid-filled supports ensured mechanical stability while minimizing material;
- Tree-like geometry simplified post-processing and avoided enclosed powder traps;
- Significant support volume reduction, though the exact savings were not quantified numerically.

Overall, the custom supports were better integrated into the part's geometry, easier to remove, and more reliable in preventing thermal distortions during the print. This strategy was a key enabler for successful simulation and real-world manufacturability.

### 3.3. Manual Geometry Refinement

Although the topology optimization delivered a structurally efficient bracket, the resulting geometry included regions that were not inherently printable without support material. Since the optimization was performed without manufacturing constraints, some areas featured overhangs that would require difficult-to-remove supports. To address this, a series of manual modifications were applied in nTop to improve printability while preserving the structural integrity of the design.

Minor interventions included the addition of **small vertical walls or cylindrical features** to support overhangs in hard-to-reach regions. These elements were carefully placed to locally reduce the need for support structures in areas where automated generation would have created inaccessible or excessive supports. All modifications were **integrated using boolean union operations, followed by blending steps** to ensure a seamless transition between the original geometry and the added features.

The most significant geometric change involved **modifying the bottom surface of the bracket** in contact with the build plate. After smoothing, this region had a slightly rounded profile, which would have required a ring of delicate support structures around its perimeter. To eliminate this issue and improve first-layer adhesion, a **section cut was taken at 5.5 mm from the base**, and the resulting flat profile was **extruded downward** to the build plate. This created a larger, planar contact surface, reduced support requirements, and ensured better thermal conduction during printing.

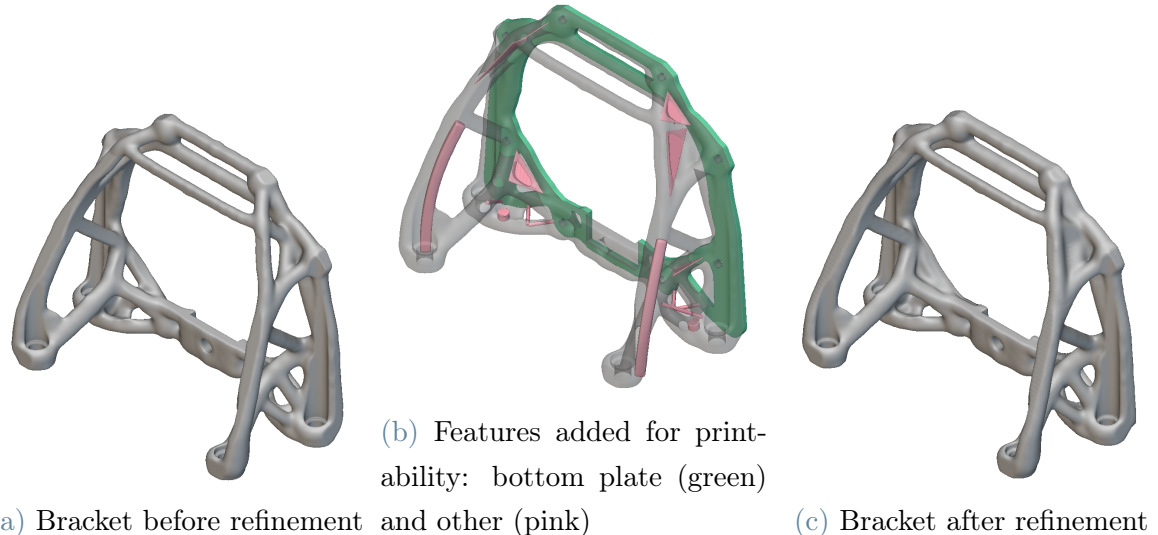


Figure 3.5: Results of manual refinement

These manual edits were crucial in converting the raw optimization output into a print-ready design with minimized support requirements and simplified post-processing, without compromising the bracket's functional or structural performance.

### 3.4. Post-DfAM Performance Validation

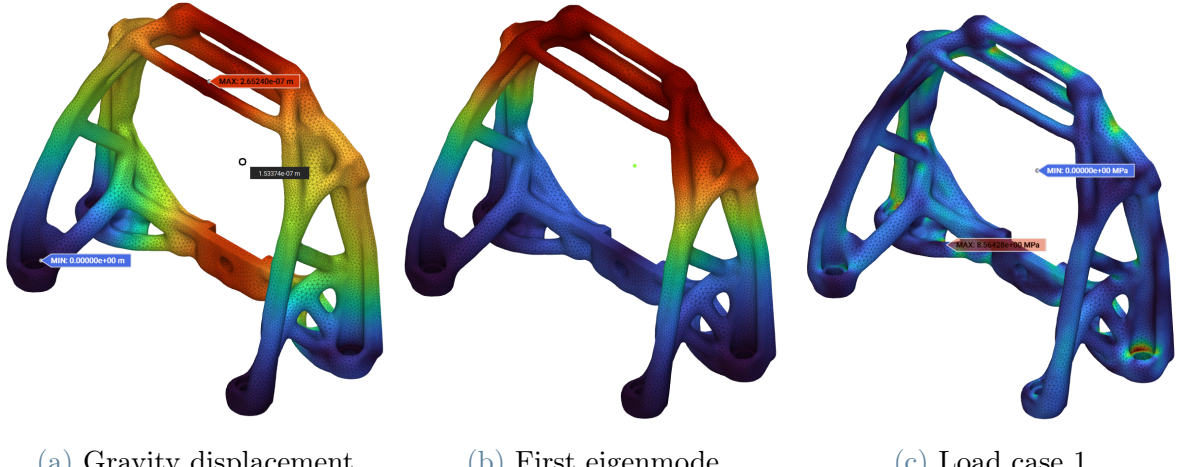
Following the manual geometry refinement described in the previous section, a final round of structural validation was performed to ensure that the design modifications did not compromise the functional requirements. This analysis used the same tools, boundary conditions, and load cases as applied during the initial topology optimization stage, enabling a direct comparison with the pre-refinement results.

The refined geometry exhibited a **mass increase from 2982 g to 3234 g**, corresponding to an 8.5% increase. This was primarily due to the addition of support-reducing features and the extruded base surface designed to improve build plate contact.

Despite the increased mass, the final design comfortably exceeded the performance criteria. The **first natural frequency rose to 399 Hz**, remaining well above the 380 Hz requirement. The maximum von Mises stresses across the four load cases remained low, with the **highest stress value being 8.78 MPa**, indicating a large safety margin:

Load Case	Peak Stress after TopOpt [MPa]	Peak Stress after DfAM [MPa]
1	6.14	8.78
2	5.84	6.46
3	6.57	7.72
4	6.16	6.40

Table 3.1: Results of quasi-static analyses



(a) Gravity displacement

(b) First eigenmode

(c) Load case 1

Figure 3.6: Results of quasi-static analysis

The displacement under gravity was also verified, yielding a maximum of 0.26 microns, far below the 5  $\mu\text{m}$  threshold.

Overall, the refinement led to a modest mass penalty but provided substantial benefits in terms of printability and manufacturability, while maintaining — and in some cases slightly improving — structural performance. The post-DfAM design thus represents a well-balanced compromise between mechanical efficiency and additive manufacturing constraints.

# 4 | Process Simulation

## 4.1. Simulation Objectives

The primary objective of the printing process simulation was to evaluate the thermal distortion and residual stresses induced during the additive manufacturing process of the redesigned bracket. Understanding these effects was critical not only to validate the design's printability but also to assess whether the strategies employed in earlier stages — such as the chosen build orientation, support minimization workflow, and geometry refinements — were effective in reducing manufacturing-induced deformation.

By incorporating the custom-designed support structures developed in the DfAM stage, the simulation aimed to provide a realistic representation of the printing scenario. This allowed the team to quantify deformation trends at critical locations (notably the satellite mounting interfaces) and determine whether they fell within acceptable limits for post-processing and final assembly.

In addition to evaluation, the simulation results were used to drive a compensation step, in which specific distortions were preemptively corrected in the geometry. This iterative approach ensured that the as-printed part would closely match the intended design once cooled and released from the build plate.

## 4.2. Simulation Setup

The printing process simulation was conducted using **Altair Inspire Print3D**, configured to reflect the manufacturing conditions of the **EOS M400 system with a 30 µm layer height**. The geometry was imported in two parts: the bracket in STEP format and the custom-designed support structures in 3MF format. This separation allowed precise treatment of support behavior and alignment with the original build layout.

A **standard AlSi10Mg material preset** provided by the software was used, without modification to thermal or mechanical parameters. Similarly, the **default machine profile and scan strategy** were retained, as the focus was not on fine-tuning process parameters but on evaluating geometry response under a representative build scenario.

The simulation used a **3 mm voxel mesh** resolution, striking a balance between accuracy and computational efficiency. A full slice-by-slice simulation was performed, modeling both the thermal build-up during layer deposition and the springback behavior after cooling and support removal.

Although the real support structures featured an internal gyroid lattice, this level of detail was not feasible to simulate directly. Therefore, **supports were modeled as solid elements**, providing an overestimate of stiffness and heat conduction.

The simulation outputs of primary interest included thermal displacement fields to identify the magnitude and location of deformation and residual stress maps to assess internal stresses that could affect part integrity or dimensional stability post-print.

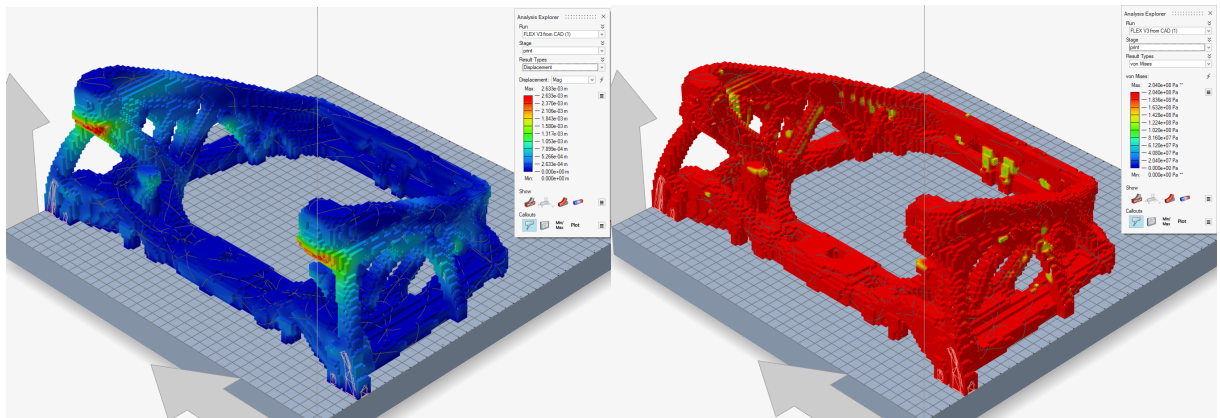
### 4.3. Deformation Results

The simulation revealed that the **most significant thermal distortions occurred at the two satellite mounting interfaces furthest from the build plate**. During the build process, maximum **displacement reached 2.64 mm**, primarily on the underside of these interfaces, where the custom support structures were attached. **After cooling and removal of supports, this displacement increased further to a peak of 3.43 mm**, confirming that post-build springback effects significantly affect the dimensional accuracy of the bracket.

**Residual stress distribution** during the build process was found to be relatively uniform, with a **maximum value of 204 MPa**. Following cooling and support removal, the stresses partially relaxed in thicker structural regions, reducing to a range of 100–150 MPa, though localized peaks of 204 MPa persisted in constrained or high-load areas. These values, while within acceptable material limits, highlighted the importance of carefully planning support placement and part orientation.

Due to the magnitude of deformation, **geometric compensation was deemed necessary**. Altair Inspire Print3D's built-in springback compensation tool was used to pre-distort the model so that, after cooling, the part would match the intended nominal geometry. Although the compensated model was not re-simulated, the earlier structural validations were assumed to remain valid, as the compensation targeted distortion only and did not significantly alter load-bearing features.

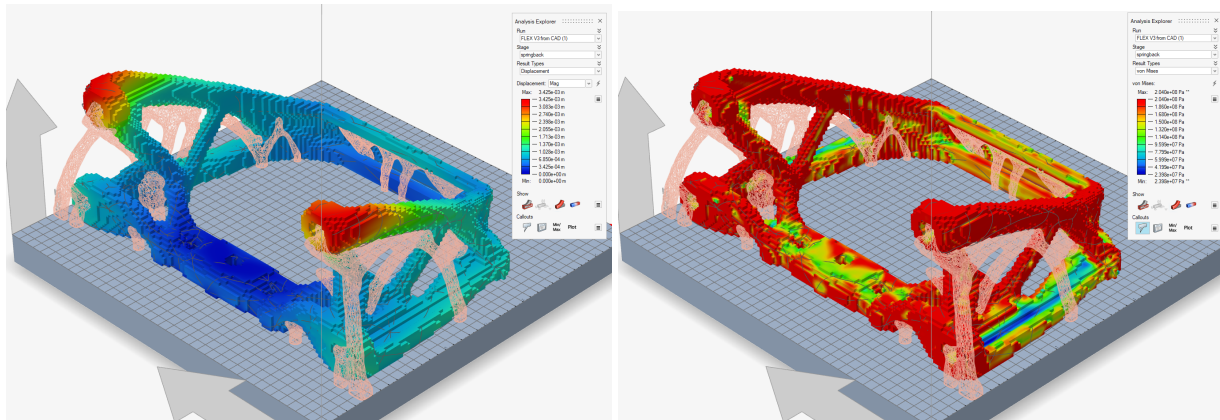
This stage confirmed that while the bracket was manufacturable in its current form, thermal distortion was non-negligible and had to be actively addressed to preserve critical interface alignment.



(a) Displacement field

(b) Von Mises stress map

Figure 4.1: Printing simulation results



(a) Displacement field

(b) Von Mises stress map

Figure 4.2: Springback simulation results

# 5 | Results Discussion and Conclusions

This project addressed the redesign of a satellite optical sensor bracket for additive manufacturing, with the overarching goal of reducing mass while satisfying demanding structural and functional requirements. Through an iterative workflow combining **topology optimization, design for additive manufacturing (DfAM), and process simulation**, we achieved a significant reduction in mass — from the original **3.7 kg to 3.2 kg** — while ensuring mechanical performance and printability.

The **topology optimization phase** proved highly effective in generating a lightweight, truss-like structure that distributed material efficiently around critical load paths. The most influential constraint in this stage was the **natural frequency requirement of 380 Hz**, which directly limited how aggressively mass could be reduced. Representing the mirror mass flexibly in the dynamic analysis ensured realistic results, especially compared to earlier trials using fully rigid couplings.

Post-optimization, the **DfAM process** was pivotal. We strategically selected a **horizontal build orientation**, confirmed via a **custom nTop-based orientation study** involving 2000 samples. **Custom support structures were designed through a second topology optimization**, which minimized compliance under gravity loading while respecting overhang and feature constraints. This novel approach resulted in supports that were both mechanically sound and easier to remove, overcoming limitations encountered with commercial support generation tools.

**Manual refinement** of the bracket geometry further enhanced manufacturability. Minor adjustments to eliminate unsupported overhangs and increase build-plate contact area contributed to a cleaner and more stable build. While these changes increased the mass slightly, from 2982 g to 3234 g, the final design still exceeded initial expectations.

**Simulation of the printing process** confirmed the necessity of springback compensation, as **deformations up to 3.43 mm** were observed in unsupported regions of the bracket. Using the **compensation tools** in Altair Inspire Print3D allowed us to pre-distort the geometry, ensuring dimensional accuracy post-build. Although the compensated model was not re-validated structurally, the assumption that mechanical performance would remain within previously validated bounds was considered reasonable.

In conclusion, the project successfully demonstrated how a complex structural component can be re-engineered for metal additive manufacturing, meeting aerospace-grade constraints. The integration of topology optimization, DfAM, and process simulation

proved critical in navigating the intricate trade-offs between **performance, printability, and manufacturability**.

Future improvements could include:

- Physical printing and dimensional validation of the compensated model;
- Testing alternative support lattice infills to reduce mass further;
- Deeper exploration of thermal control strategies during printing to reduce residual stress formation.

Overall, the approach developed here provides a replicable framework for similar redesign challenges in aerospace and other high-performance sectors.

Parameter	Value	Requirement
Mass	$3.234\text{kg}$	$< 3.7\text{kg}$
First eigenfrequency	$399\text{Hz}$	$> 380\text{Hz}$
Max mirror displacement	$0.15\mu\text{m}$	$< 5\mu\text{m}$
Static Yield SF (vertical)	26 (Load 1)	-
Support mass	$0.343\text{kg}$	-
Max thermal distortion	$3.43\text{mm}$	-

Table 5.1: Summary of the Final Bracket